SSRG International Journal of Electrical and Electronics Engineering
ISSN: 2348-8379/ https://doi.org/10.14445/23488379/IJEEE-V10I1P116

Volume 10 Issue 1, 168-175, January 2023

Original Article

Hybrid LSTM/GRU-based Domain Adaptation Model for Correlation Analysis to Detect Glaucoma

Deepali M. Kotambkar[1], Pallavi M. Wankhede[2]

[1]*Department of Electronics Engineering Department, Shri Ramdeobaba College of Engineering and Management, Nagpur*

[2]*Deparment of Computer Engineering Department, St Vincent Pallotti College of Engineering and Technology, Nagpur*

[1]*Corresponding Author : shelkedt@rknec.edu*

Received: 07 December 2022 Revised: 13 January 2023 Accepted: 19 January 2023 Published: 29 January 2023

Abstract *- Glaucoma identification is a multidomain task which involves the analysis of multimodal report sets. These sets include retinal scans from different sensors, blood report parameters, and eyesight reports. Existing glaucoma identification models either use a single report for analysis or suffer from domain adaptation issues, which limits their classification performance. Moreover, the models that use multidomain scans are highly complex and thus have limited scalability levels. To overcome these issues, the study of this text proposes the design of a hybrid Long-Short-Term Memory (LSTM) with a Gated Recurrent Unit (GRU) to identify glaucoma via correlation analysis. Both LSTM & GRU are individually capable of representing any signal into feature sets, but a hybrid combination of these models assists in the optimal representation of retinal reports via high-density feature analysis. These features are selected via a Genetic Algorithm (GA), which uses inter-class feature variation for fitness optimizations. The selected features are processed via a classification model that uses dual Convolutional Neural Networks (dCNNs) and assists in incorporating transfer learning during classification operations. The dCNN comprises a Recurrent Neural Network (RNN), which performs the initial classification of individual scans into approximate glaucoma levels. These approximate levels are fine-tuned by a customized CNN, which assists in identifying final glaucoma severity under clinical use cases. Correlation analysis between retinal scan components (including Macula, Arteries, Veins, and Optical Disc features) and glaucoma-specific blood reports & eyesight reports assist in continuous optimizations. Due to these operations, the proposed model can achieve 8.5% higher accuracy, 9.3% higher precision, and 4.9% higher recall, with 12.5% lower computational delay when compared with existing methods. These observed enhancements assist in deploying the model for real-time clinical use cases.*

Keywords *- GRU, LSTM, GA, RNN, CNN, Macula, Veins, Optical Disc, Arteries.*

1. Introduction

Deep convolutional neural networks (DCNNs) have the ability to acquire efficient representations that are typically relevant to a number of applications and visual domains when trained on large-scale datasets [1–10]. However, classification models trained using the representations of a single dataset perform less well on additional datasets and classification tasks with Deep Relation Transformers (DRT) [1, 10]. This is due to an issue known as dataset bias or domain shift [11]. To further fine-tune these models, it is customary to use datasets specific to the task at hand. Nonetheless, getting sufficient labelled data to precisely alter a large number of the parameters required by deep multi-layer networks may be difficult and costly.[12-20] The objective of domain adaptation strategies is to offset the negative effects of domain changes. In more recent domain adaptation algorithms, transformations that turn the source and target domains into a single latent feature space are being learned. Commonly, this is accomplished by optimizing the representations to reduce a domain shift indicator, such as the maximum mean discrepancy [22, 29] or the correlation distances [16, 19]. Presented here [21] is a method for effectively recreating the target domain from its source representation. In recent years, the generative adversarial adaptation method has gained popularity as an example of this principle. To lower the approximate domain discrepancy distance, this strategy employs an adversarial goal in connection to a domain discriminator. Generally, generative adversarial learning is closely related to adversarial adaptation [22], which pits the generator against the discriminator. This kind of learning needs competition between the generator and discriminator. The technique by which the generator creates its pictures deceives the discriminator, which strives to distinguish between synthetic and genuine photographs. This causes the discriminator's task to fail. In the realm of domain adaptation, this idea has been used to guarantee that the network cannot differentiate between the distributions of

data originating from its source domain and data originating from its target domain via Self-Organized Operational Neural Networks (Self-ONNs) [19], [23], [24]. In contrast, these algorithms must make design decisions, such as which loss function to use, whether or not to utilize a generator, and whether or not to share weights between domains. For instance, although [24] divides some layers to train a slightly asymmetric mapping, [27] and [29] [31] share weights and learn a symmetric mapping of both the source and target images into a single feature space by sharing weights. This is achieved by mapping both the source and target images to the same feature space. Nevertheless, there are currently no effective domain adaptation algorithms that can adapt to fundus photographs for the purpose of glaucoma diagnosis. [25,26] In general, fundus images may be acquired utilizing a variety of medical equipment, but the photographs nearly always have the same basic look. In part, different sets of fundus pictures may be distinguished from one another based on the location of the optic disc and optic cup. The most noticeable distinction between this set and the others is the overall brightness. Since pictures of the optic disc and cup of the fundus may be analyzed to detect glaucoma, these alterations are not an essential feature in an ophthalmologist's glaucoma diagnosis. In contrast, these changes significantly impacted classification when it came to models of classification that were trained on several datasets.[28]

This experimental study provides a hybrid LSTM and GRU-based Domain Adaptation Model for Correlation Analysis-based Glaucoma Diagnosis within the scope of this work. Moreover, to properly represent feature sets, our technique combines LSTM and GRU. The majority of the proposed model consists of two distinct models. The first is an unsupervised Genetic Algorithm (GA) for feature selection, while the second is a source-photograph-based, pre-trained classification model. Both of these models need picture inputs. Here a new domain adaption strategy that employs deep convolutional neural networks (dCNNs) for transfer learning operations is presented. This work provides a novel technique for extracting and selecting glaucoma-related characteristics. In addition, we contribute to enhancing classification performance for multimodal report types by developing a correlation model. Our efforts have been beneficial in various application contexts, as seen by the outcomes gained from a number of medical imaging clinical image sets.[30]

2. Proposed Methodology

Based on the review of existing glaucoma analysis models, it can be observed that these models either use a single report for analysis or suffer from domain adaptation issues, which limits their classification performance. Moreover, the models that use multidomain scans are highly complex and thus have limited scalability levels. To overcome these issues, this section proposes the design of a hybrid Long-Short-Term Memory (LSTM) with Gated Recurrent Unit (GRU) to identify glaucoma via correlation analysis.

As observed from Fig 1, both LSTM & GRU are individually capable of representing any signal into feature sets, but a hybrid combination of these models assists in the optimal representation of retinal reports via high-density feature analysis. These features are selected via a Genetic Algorithm (GA), which uses inter-class feature variation for fitness optimizations. The selected features are processed via a classification model that uses dual Convolutional Neural Networks (dCNNs) and assists in incorporating transfer learning during classification operations. The dCNN comprises a Recurrent Neural Network (RNN), which performs the initial classification of individual scans into approximate glaucoma levels. These approximate levels are fine-tuned by a customized CNN, which assists in identifying final glaucoma severity under clinical use cases. Correlation analysis between retinal scan components (including Macula, Arteries, Veins, and Optical Disc features) and glaucoma-specific blood reports & eyesight reports assist in continuous optimizations.

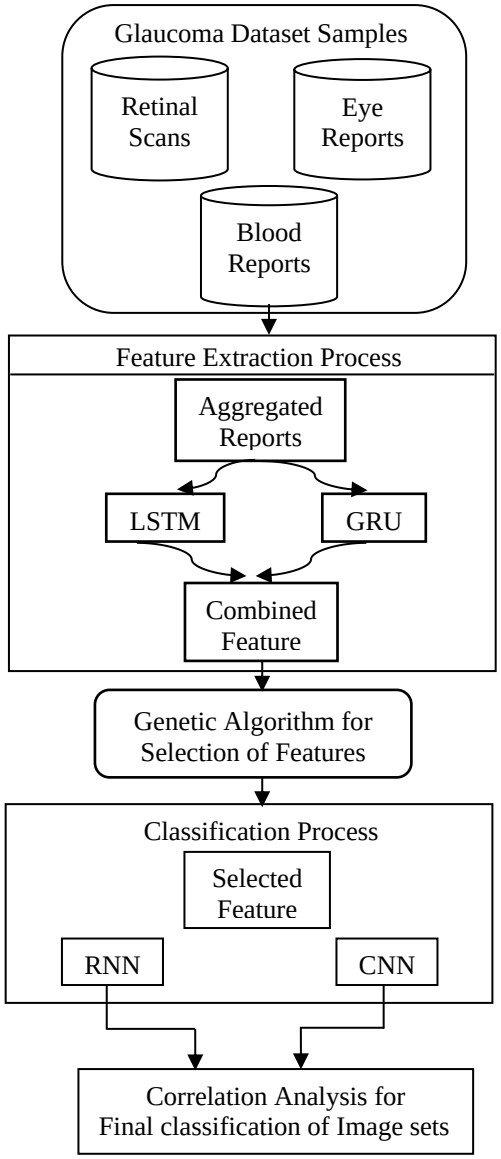

Fig. 1 Flow diagram of the proposed model for Glaucoma classifications

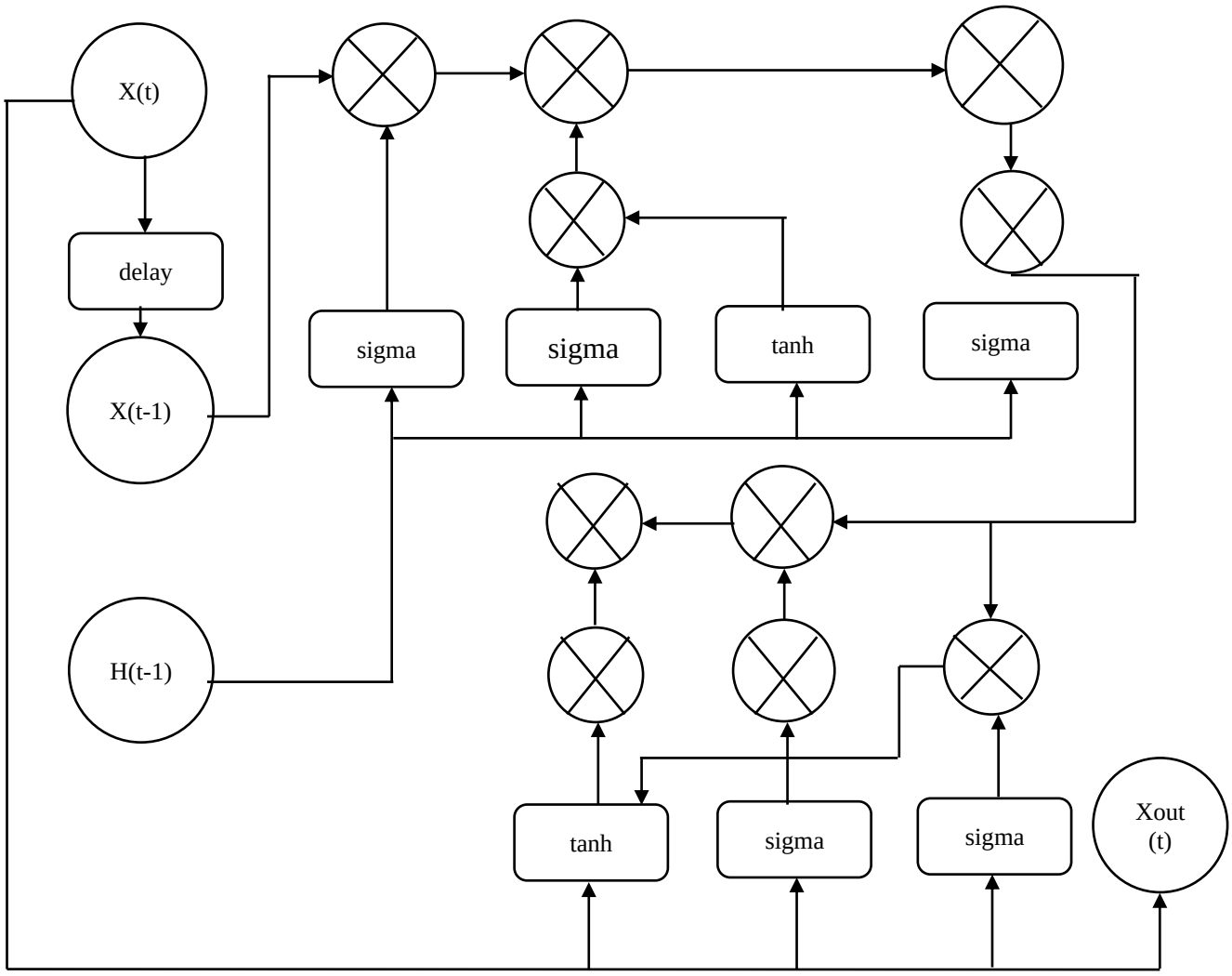

Fig. 2 Hybrid LSTM & GRU-based model for extraction of features

3. Hybrid LSTM & GRU Model

The initial reports from the data set are aggregated and given to an efficient hybrid LSTM & GRU-based feature extraction model, which is depicted in Fig 2.

Due to this combination, the model can identify high-density feature sets. These sets are initially extracted via equations 1, 2, 3, 4, 5 and 6 as follows,

$$i = var(x_{in} * U^{i} + h_{t-1} * W^{i}) \dots\dots\dots\dots \quad (1)$$

$$f = var\left(x_{in} * U^{f} + h_{t-1} * W^{f}\right) \dots\dots\dots\dots \quad (2)$$

$$o = var(x_{in} * U^{o} + h_{t-1} * W^{o}) \dots\dots\dots\dots \quad (3)$$

$$C'_{t} = \tanh(x_{in} * U^{g} + h_{t-1} * W^{g}) \dots\dots\dots \quad (4)$$

$$T_{out} = var(f_{t} * x_{in}(t-1) + i * C'_{t}) \dots\dots\dots \quad (5)$$

$$h_{out} = \tanh(T_{out}) * o \dots\dots\dots\dots \quad (6)$$

Where, x_{in}, W & *U* represents aggregated input reports and LSTM constants, which are set up by the hyperparameter tuning process. The extracted features are further augmented via the use of an efficient GRU-based model, which can be represented via equations 7, 8, 9 and 10 as follows,

$$z = var(W_{z} * [h_{out} * T_{out}]) \dots\dots\dots\dots \quad (7)$$

$$r = var(W_{r} * [h_{out} * T_{out}]) \dots\dots\dots\dots \quad (8)$$

$$h'_{t} = \tanh(W * [r * h_{out} * T_{out}]) \dots\dots\dots\dots \quad (9)$$

$$xout = (1-z) * h'_{t} + z * h_{out} \dots\dots\dots\dots \quad (10)$$

Where, W represents the GRU constant, which is tuned similarly to LSTM constants. The output feature sets xout are selected via a Genetic Algorithm (GA) based model, which works as per the following process. The output feature sets xout are selected via a Genetic Algorithm (GA) based model, which works as per the following process,

To initialize the feature selection process, setup the following GA constants,

- Total optimization iterations (N_i)
- Total optimization solutions (N_s)
- Rate of learning (L_r)

Generate N_s solutions via the following process,

- Select N features via equation 11,

$$N = STOCH(L_r * N_f, N_f) \dots\dots\dots\dots\dots\dots\dots (11)$$

Where, STOCH represents a stochastic Markovian process, while N_f represents total features extracted by the combined LSTM & GRU process.

The selected features are used to find the fitness levels of the current solution via equation 12,

$$f = \frac{\sum_{i=1}^{N} x_i - \frac{\sum x}{N}}{N} \dots\dots\dots\dots\dots\dots\dots (12)$$

Where, x represents the intensity of feature values that are extracted via the LSTM & GRU process.

- Once these values are generated then, a fitness threshold is estimated via equation 13,

$$f_{th} = \sum_{i=1}^{N_s} f_i * \frac{L_r}{N_s} \dots\dots\dots\dots\dots\dots\dots\dots (13)$$

- After this evaluation, modify all solutions with$f < f_{th}$, while passing other solutions to the next iterations.
- This process is repeated for N_i iterations and the solution with maximum fitness are selected for further classification operations.

The selected features are initially classified via an RNN-based model, which uses 'purelin' based activations via equation 14 to identify Glaucoma levels,

$$C_{out} = \text{purelin}\left(\sum_{i=1}^{N} xout_i * W_i\right) \dots\dots\dots\dots\dots\dots (14)$$

Where, $xout \& W_i$ represents the features selected by the GA process and weights tuned via the RNN classification process. These features are also classified via an efficient CNN model, which can be observed in figure 3, wherein Convolutional, Max Pooling, and Drop Out layers are combined with the Fully Connected Layer to obtain final Glaucoma classes. The model extracts convolutional features via equation 15,

$$Conv_{out_i} = \sum_{a=-\frac{m}{2}}^{\frac{m}{2}} xout(i-a) * \text{ReLU}\left(\frac{m}{2} + a\right) \dots\dots\dots\dots (15)$$

Where, m & a represents window size and stride size for the convolutions, while ReLU represents a rectilinear unit which is used for activation of extracted feature sets. The window and stride sizes are varied between 1x64 to 1x512, which assists in extracting large feature sets.

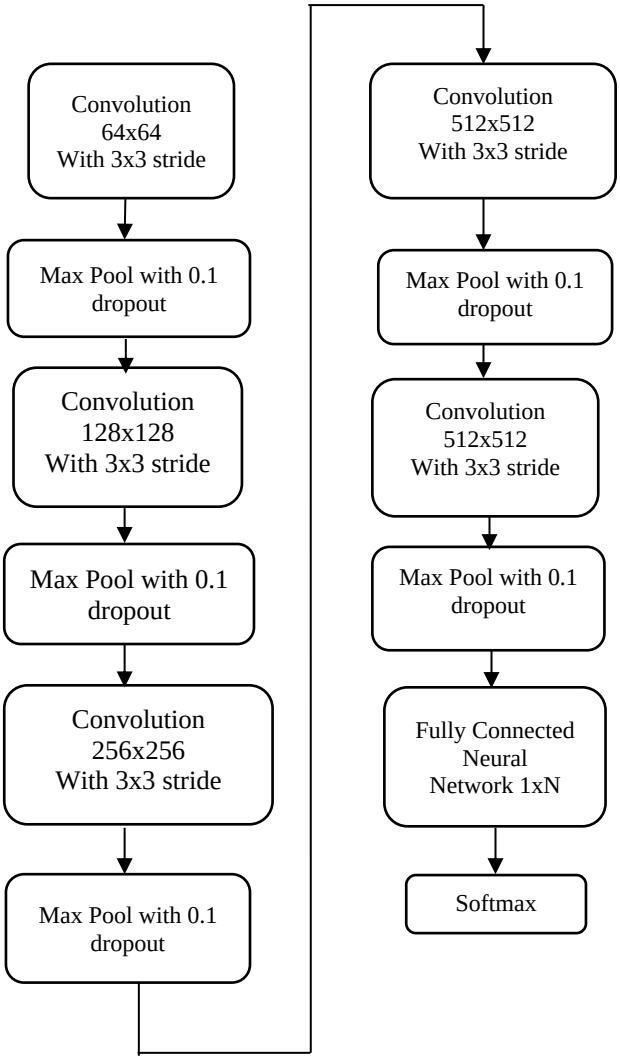

Fig. 3 Design of the proposed CNN Model for identification of Glaucoma levels

4. Result Analysis & Comparison

The proposed model uses a combination of LSTM & GRU for feature extraction, cascaded with GA to identify highly variant feature sets. The selected sets are classified via a combination of CNN and RNN, which assists in identifying Glaucoma levels. For different dataset samples, these levels are estimated for multiple retinal components, including Macula, Arteries, Veins, and Optical Disc. These dataset samples were taken from the following sources,

- OCT Scans from Kaggle
- PAPILA
- RIGA

The model's performance was compared w.r.t. accuracy (A), precision (P), recall (R), and delay (D) levels, which were evaluated via equations 19, 20, 21, and 22 as follows,

$$A = \frac{t_p + t_n}{t_p + t_n + f_p + f_n} \dots\dots\dots (19)$$

$$P = \frac{t_p}{t_p + f_p} \dots\dots\dots\dots \quad (20)$$

$$R = \frac{t_p}{t_p + t_n + f_p + f_n} \dots\dots\dots\dots (21)$$

$$d = \frac{1}{N}\sum_{i=1}^{N} t_{end_i} - t_{start_i} \dots\dots\dots\dots\dots (22)$$

Where, $t_p, f_p, t_n \& f_n$ represent usual true & false identification rates, while $t_{end} \& t_{start}$ are timestamps during the start & completion of the classification process. A total of 25k samples were used for evaluation, out of which 75% were used for training, 15% for testing &10% for validation operations. Using these sets, the accuracy can be observed from table 1, where it was compared with Glau Net [1], DRT [10], and Self ONN [19], w.r.t. different Test Image Sets (TIS) as follows,

Table 1. Accuracy of Glaucoma Analysis

TIS	A (%) Glau Net [1]	A (%) DRT [10]	A (%) Self ONN [19]	A (%) This Work
1108	81.11	86.92	88.63	97.57
2225	81.16	87.23	88.83	97.65
3333	81.21	87.53	89.02	97.73
4442	81.26	87.84	89.21	97.80
5558	81.31	88.16	89.40	97.85
6667	81.36	88.48	89.59	97.90
7775	81.41	88.81	89.79	97.94
8892	81.47	89.14	90.00	97.98
10000	81.52	89.47	90.21	98.02
11108	81.57	89.79	90.42	98.06
12225	81.62	90.10	90.63	98.11
13892	81.67	90.42	90.84	98.16
16667	81.72	90.74	91.04	98.21
18058	81.78	91.05	91.24	98.27
19442	81.83	91.37	91.44	98.34
22225	81.88	91.68	91.63	98.40
23608	81.93	92.00	91.83	98.47
25000	81.99	92.32	92.03	98.54

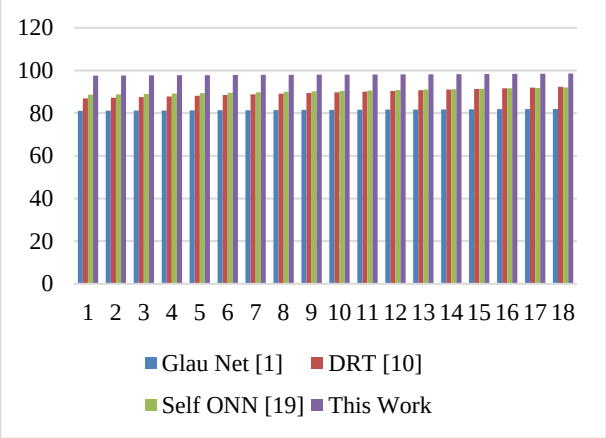

Fig. 4 Accuracy of Glaucoma analysis

Fig. 4 illustrates the results of these tests, showing that the suggested classification model can outperform Glau Net [1] by 15.5%, DRT [10] by 6.4%, and Self ONN [19] by 6.5% in terms of accuracy. Therefore, it is applicable to a broad range of categorization problems that occur in real-time. This is achieved by using a dCNN-based classification technique in conjunction with hybrid LSTM and GRU networks and a high-density feature extraction process. Similarly, the precision of classification was evaluated in table 2 as follows,

Table 2. The precision of glaucoma analysis

TIS	P (%) Glau Net [1]	P (%) DRT [10]	P (%) Self ONN [19]	P (%) This Work
1108	79.20	83.21	85.71	96.49
2225	79.25	83.51	85.90	96.55
3333	79.30	83.81	86.08	96.61
4442	79.36	84.12	86.26	96.66
5558	79.41	84.43	86.45	96.71
6667	79.46	84.74	86.64	96.75
7775	79.51	85.05	86.84	96.79
8892	79.56	85.36	87.05	96.83
10000	79.61	85.67	87.25	96.87
11108	79.66	85.97	87.44	96.92
12225	79.71	86.27	87.64	96.97
13892	79.76	86.57	87.83	97.02
16667	79.81	86.87	88.02	97.08
18058	79.86	87.17	88.21	97.14
19442	79.91	87.47	88.40	97.20
22225	79.96	87.77	88.59	97.26
23608	80.01	88.07	88.78	97.30
25000	80.06	88.38	88.98	97.35

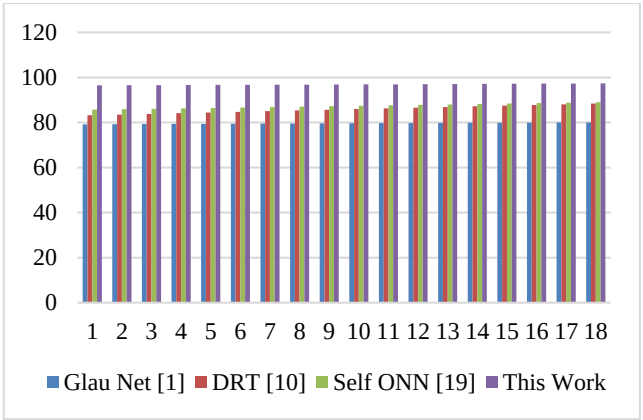

Fig. 5 The precision of Glaucoma analysis

Fig 5 summarizes the results of these analyses and shows that the suggested classification model outperforms Glau Net [1] by 18.3%, DRT [10] by 9.1%, and Self ONN [19] by 8.5% in terms of precision. As a result, it is applicable to a broad range of categorization tasks in real-time. That's because we employed LSTM and GRU for feature extraction, GA for feature selection, dCNN for classification, and efficient segmentation techniques. Similarly, recall of classification was evaluated in table 3 as follows,

Table 3. Recall of glaucoma analysis

TIS	R (%) Glau Net [1]	R (%) DRT [10]	R (%) Self ONN [19]	R (%) This Work
1108	78.22	85.22	86.19	95.86
2225	78.27	85.52	86.38	95.93
3333	78.32	85.82	86.56	96.00
4442	78.37	86.13	86.75	96.05
5558	78.42	86.45	86.94	96.10
6667	78.47	86.77	87.13	96.15
7775	78.53	87.07	87.32	96.19
8892	78.61	87.32	87.51	96.25
10000	78.70	87.55	87.70	96.32
11108	78.79	87.77	87.87	96.39
12225	78.88	87.99	88.05	96.46
13892	78.97	88.24	88.23	96.54
16667	79.05	88.48	88.40	96.61
18058	79.13	88.71	88.58	96.69
19442	79.21	88.97	88.76	96.77
22225	79.27	89.24	88.94	96.83
23608	79.34	89.53	89.13	96.89
25000	79.39	89.83	89.32	96.94

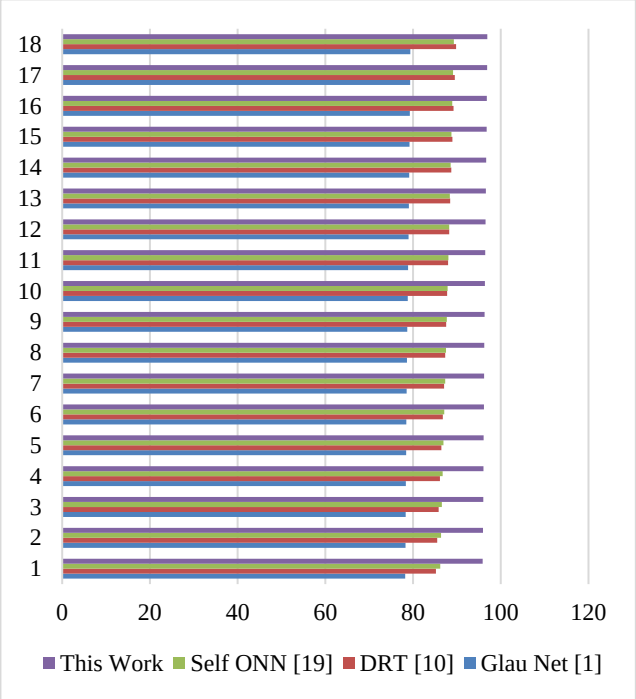

Fig. 6 Recall of Glaucoma analysis

When one considers these evaluations and observes figure 6, it becomes abundantly evident that the suggested classification model can provide recall outcomes that are, respectively, 16.5%, 8.3%, and 8.5% superior to those generated by Glau Net [1], DRT [10], and Self ONN [19]. As a consequence of this, it performs very well in a wide range of real-time categorization settings. This is because well-established segmentation approaches were combined with dense feature extraction and ensemble classification to achieve this result. Similarly, the delay of classification was evaluated in table 4 as follows,

Table 4. Delay needed for glaucoma analysis

TIS	D (ms) Glau Net [1]	D (ms) DRT [10]	D (ms) Self ONN [19]	D (ms) This Work
1108	111.31	102.14	104.22	103.55
2225	111.38	102.50	104.44	103.62
3333	111.45	102.86	104.67	103.69
4442	111.53	103.23	104.89	103.76
5558	111.60	103.61	105.12	103.81
6667	111.67	104.00	105.35	103.86
7775	111.74	104.39	105.59	103.90
8892	111.81	104.77	105.83	103.94
10000	111.88	105.14	106.08	103.98
11108	111.95	105.52	106.32	104.03
12225	112.02	105.89	106.56	104.08
13892	112.09	106.26	106.80	104.14
16667	112.17	106.63	107.03	104.20
18058	112.24	107.00	107.26	104.26
19442	112.31	107.37	107.50	104.33
22225	112.38	107.74	107.73	104.39
23608	112.45	108.11	107.96	104.44
25000	112.52	108.49	108.20	104.50

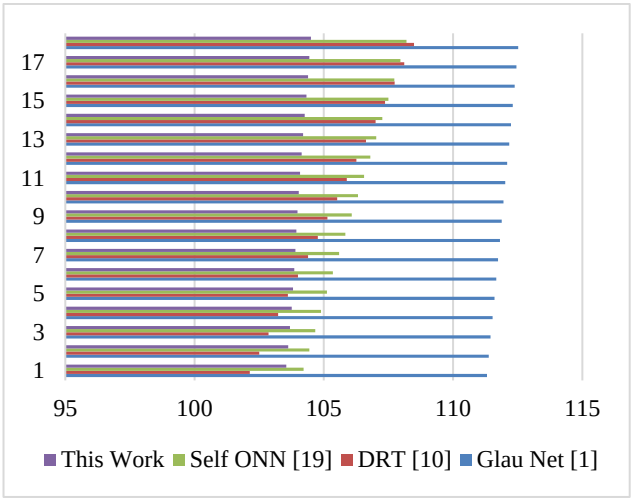

Fig. 7 Delay needed for Glaucoma analysis

When compared to the delays created by Glau Net [1], DRT [10], and Self ONN [19], it is clear that the suggested categorization model is capable of producing delays that are, respectively, 8.5 percent, 4.9 percent, and 4.5 percent shorter. This can be seen clearly when looking at Figure 7. As a consequence of this, it performs very well in a wide range of real-time categorization settings. This is because, after the segmentation process has been completed successfully, high-density feature extraction and ensemble classification are used. The created model proved useful in a range of contexts involving the categorization of glaucoma phases as a result of these enhancements, which were included in the model for efficient analysis.

5. Conclusion and Future Scope

The proposed model extracts feature using a mix of LSTM and GRU, which are then cascaded using GA to identify highly varied feature sets. The chosen sets are categorized using a CNN and RNN combination to

identify the degrees of glaucoma. These values are calculated for the Macula, Arteries, Veins, and Optical Disc, among other retinal components for various dataset samples. The classification model can perform more accurately than Glau Net [1] by 15.5%, DRT [10] by 6.4%, and Self ONN [19] by 6.5%, according to an accuracy assessment. As a result, it may be used to solve various real-time classification issues. This is accomplished by combining a dCNN-based classification approach with hybrid LSTM and GRU networks, high-density feature extraction, and LSTM and GRU networks. In terms of accuracy, the proposed classification model surpasses Glau Net [1] by 18.3%, DRT [10] by 9.1%, and Self ONN [19] by 8.5%.

As a consequence, it may be used in real-time for a variety of classification jobs. That's because we used effective segmentation methods, dCNN for classification, LSTM and GRU for feature extraction, and GA for feature selection. The recall results produced by the proposed classification model are, respectively, 16.5%, 8.3%, and 8.5% better than those produced by Glau Net [1], DRT [10], and Self ONN [19]. This leads to excellent performance in a variety of real-time classification contexts. The outcome was obtained by combining well-known segmentation techniques with dense feature extraction and ensemble classification. It is obvious that the recommended categorization model is capable of providing delays that are, respectively, 8.5 percent, 4.9 percent, and 4.5 percent quicker performance levels when compared to the delays produced by Glau Net [1], DRT [10], and Self ONN [19]. This leads to excellent performance in a variety of real-time classification contexts. This is so that high-density feature extraction and ensemble classification may be employed once the segmentation procedure has been successfully finished. These improvements, which were included in the model for effective analysis, have shown to be helpful in various settings involving the classification of glaucoma stages. In future, the model must be validated for larger datasets and can be extended via low-complexity feature analysis techniques, which will assist in improving its classification performance under multimodal sets. Researchers can also use deep learning techniques like Auto Encoders and Transformers to further optimize its performance under different dataset samples.

References

[1] Anita Manassakorn et al., "Glaunet: Glaucoma Diagnosis for OCTA Imaging Using A New CNN Architecture," *IEEE Access*, vol. 10, pp. 95613-95622, 2022, *Crossref,* https://doi.org/10.1109/ACCESS.2022.3204029

[2] R. Tamilaruvi et al., "Brain Tumor Detection in MRI Images Using Convolutional Neural Network Technique," *SSRG International Journal of Electrical and Electronics Engineering*, vol. 9, no. 12, pp. 198-208, 2022. *Crossref,* https://doi.org/10.14445/23488379/IJEEE-V9I12P118

[3] Jiyeon Kim et al., "Feature Analysis of IoT Botnet Attacks Based on RNN and LSTM," *International Journal of Engineering Trends and Technology*, vol. 68, no. 4, pp. 43-47, 2020. *Crossref,* https://doi.org/10.14445/22315381/IJETT-V68I4P208S

[4] Patthapol Kunumpol et al., "Glaucutu: Time Until Perceived Virtual Reality Perimetry with Humphrey Field Analyzer Prediction-Based Artificial Intelligence," *IEEE Access*, vol. 10, pp. 36949-36962, 2022, *Crossref,* https://doi.org/10.1109/ACCESS.2022.3163845

[5] Wheyming Tina Song, Ing-Chou Lai, and Yi-Zhu Su, "A Statistical Robust Glaucoma Detection Framework Combining Retinex, CNN, and DOE Using Fundus Images," *IEEE Access*, vol. 9, pp. 103772-103783, 2021. *Crossref,* https://doi.org/10.1109/ACCESS.2021.3098032

[6] Devangjani, and Anandmankodia, "A Novel Approach for Real Time Multi-Scene Violent Activities Recognition with Modified Resnet50 and LSTM," *International Journal of Engineering Trends and Technology*, vol. 70, no. 8, pp. 292-309, 2022. *Crossref,* https://doi.org/10.14445/22315381/IJETT-V70I8P231

[7] Deepak Parashar, and Dheeraj Agrawal, "2-D Compact Variational Mode Decomposition- Based Automatic Classification of Glaucoma Stages from Fundus Images," *IEEE Transactions on Instrumentation and Measurement*, vol. 70, pp. 1-10, 2021, *Crossref,* https://doi.org/10.1109/TIM.2021.3071223

[8] Megha V. Gupta, and Shubhangi L. Vaikole, "A Parallel Fusion RNN-LSTM Approach to Classify Mental Stress Using EEG Data," *International Journal of Engineering Trends and Technology*, vol. 70, no. 10, pp. 285-297, 2022. *Crossref,* https://doi.org/10.14445/22315381/IJETT-V70I10P228

[9] Murthy V. S. N. Tatavarthy, and V. Naga Lakshmi, "Pedagogical Content Knowledge Classification Using CNN with Bi-LSTM," *International Journal of Engineering Trends and Technology*, vol. 70, no. 8, pp. 264-271, 2022.*Crossref,* https://doi.org/10.14445/22315381/IJETT-V70I8P228

[10] Diping Song et al., "Deep Relation Transformer for Diagnosing Glaucoma with Optical Coherence Tomography and Visual Field Function," *IEEE Transactions on Medical Imaging*, vol. 40, no. 9, pp. 2392-2402, 2021. *Crossref,* https://doi.org/10.1109/tmi.2021.3077484

[11] D. Parashar, and D. K. Agrawal, "Automatic Classification of Glaucoma Stages Using Two-Dimensional Tensor Empirical Wavelet Transform," *IEEE Signal Processing Letters*, vol. 28, pp. 66-70, 2021, *Crossref,* https://doi.org/10.1109/LSP.2020.3045638

[12] Tianjipeng, Manasa S, and Dr. T.C.Manjunath, "Early Detection of Eye Disease in Humans Using Random forest & HOG Concepts," *SSRG International Journal of Electronics and Communication Engineering*, vol. 7, no. 4, pp. 5-7, 2020. *Crossref,* https://doi.org/10.14445/23488549/IJECE-V7I4P102

[13] Alu E. S., Aniobi D. E., and Ijah S. T., "Mobile Expert System on Febrile Diseases," *International Journal of Computer & Organization Trends*, vol. 7, no. 4, pp. 1-11, 2017.

[14] Dr. B. Sakthivel et al., "IoT Based Solar Power Monitoring and Prediction Using Cuckoo Optimized LSTM," *International Journal of P2P Network Trends and Technology*, vol. 11, no. 2, pp. 6-8, 2021. *Crossref*, https://doi.org/10.14445/22492615/IJPTT-V11I2P402

[15] Manal Alghamdi, and Mohamad Abdel-Mottaleb, "A Comparative Study of Deep Learning Models for Diagnosing Glaucoma From Fundus Images," *IEEE Access*, vol. 9, pp. 23894-23906, 2021. *Crossref*, https://doi.org/10.1109/ACCESS.2021.305664

[16] Mir Tanvir Islam et al., "Deep Learning-Based Glaucoma Detection with Cropped Optic Cup and Disc and Blood Vessel Segmentation," *IEEE Access*, vol. 10, pp. 2828-2841, 2022, *Crossref*, https://doi.org/10.1109/ACCESS.2021.3139160

[17] Ms.S.Deepa, and Mr.S.Vijayprasath, "Certain Investigation of the Retinal Hemorrhage Detection in Fundus Images," *SSRG International Journal of Electronics and Communication Engineering*, vol. 2, no. 2, pp. 24-34, 2015. *Crossref*, https://doi.org/10.14445/23488549/IJECE-V2I2P106

[18] Poonam S. Panaskar, and Varsha D.Jadhav, "Nutritional, Antioxidant and GCMS Screening of Antidesma MONTANUM bl. Leaves," *SSRG International Journal of Medical Science*, vol. 6, no. 8, pp. 1-9, 2019. *Crossref*, https://doi.org/10.14445/23939117/IJMS-V6I8P101

[19] Ozer Can Devecioglu et al., "Real-Time Glaucoma Detection from Digital Fundus Images Using Self-Onns," *IEEE Access*, vol. 9, pp. 140031-140041, 2021. *Crossref*, https://doi.org/10.1109/ACCESS.2021.3118102

[20] Dr. R. Surendiran et al., "Effective Autism Spectrum Disorder Prediction to Improve the Clinical Traits Using Machine Learning Techniques," *International Journal of Engineering Trends and Technology*, vol. 70, no. 4, pp. 343-359, 2022. *Crossref*, https://doi.org/10.14445/22315381/IJETT-V70I4P230

[21] S. Krishnan, J. Amudha, and Sushma Tejwani, "Gaze Exploration Index (GE I)-Explainable Detection Model for Glaucoma," *IEEE Access*, vol. 10, pp. 74334-74350, 2022. *Crossref*, https://doi.org/10.1109/ACCESS.2022.3188987

[22] Quoc Cuong Ngo et al., "Pupillary Complexity for the Screening of Glaucoma," *IEEE Access*, vol. 9, pp. 144871-144879, 2021, *Crossref*, https://doi.org/10.1109/ACCESS.2021.3122079

[23] Oluwatobi Joshua Afolabi et al., "The Use of U-Net Lite and Extreme Gradient Boost (XGB) for Glaucoma Detection," *IEEE Access*, vol. 9, pp. 47411-47424, 2021, Doi: 10.1109/ACCESS.2021.3068204.

[24] Kaveri A Thakoor et al., "Robust and Interpretable Convolutional Neural Networks to Detect Glaucoma in Optical Coherence Tomography Images," *IEEE Transactions on Biomedical Engineering*, vol. 68, no. 8, pp. 2456-2466, 2021.*Crossref*, https://doi.org/10.1109/tbme.2020.3043215

[25] Tianjipeng, Suma P, and Dr. T.C.Manjunath, "AI, ML and the Eye Disease Detection," *SSRG International Journal of Computer Science and Engineering*, vol. 7, no. 4, pp. 1-3, 2020. *Crossref*, https://doi.org/10.14445/23488387/IJCSE-V7I4P101

[26] Mohammed Yesufgetu, and Husain Shahnawaz, "A Proposed Model for Health Management and Expert Diagnosis System for the Prediction of Common Diseases for Ethiopia (East Africa)," *SSRG International Journal of Medical Science*, vol. 5, no. 2, pp. 1-9, 2018. *Crossref*, https://doi.org/10.14445/23939117/IJMS-V5I2P101

[27] Ronald H Silverman et al., "High-Frequency Ultrasound Activation of Perfluorocarbon Nanodroplets for Treatment of Glaucoma," *IEEE Transactions on Ultrasonics, Ferroelectrics, and Frequency Control*, vol. 69, no. 6, pp. 1910-1916, 2022, *Crossref*, https://doi.org/10.1109/tuffc.2022.3142679.

[28] Dr. R. Surendiran et al., "Exploring the Cervical Cancer Prediction by Machine Learning and Deep Learning with Artificial Intelligence Approaches," *International Journal of Engineering Trends and Technology*, vol. 70, no. 7, pp. 94-107, 2022. *Crossref*, https://doi.org/10.14445/22315381/IJETT-V70I7P211

[29] Md. Sarwar Kamal et al., "Explainable AI for Glaucoma Prediction Analysis to Understand Risk Factors in Treatment Planning," *IEEE Transactions on Instrumentation and Measurement*, vol. 71, pp. 1-9, 2022, *Crossref*, https://doi.org/10.1109/TIM.2022.3171613

[30] Dr. R. Surendiran et al., "A Systematic Review Using Machine Learning Algorithms for Predicting Preterm Birth," *International Journal of Engineering Trends and Technology*, vol. 70, no. 5, pp. 46-59, 2022. *Crossref*, https://doi.org/10.14445/22315381/IJETT-V70I5P207

[31] Sakshi Goyal, and Deepali. M. Kotambkar, "Exploring Unet Architecture for Semantic Segmentation of the Brain MRI Scans," *Advanced Machine Intelligence and Signal Processing*, Springer, vol. 858, 2022. *Crossref*, https://doi.org/10.1007/978-981-19-0840-8_43